

Postmortem Study of Validation of Low Signal on Fat-Suppressed T1-Weighted Magnetic Resonance Imaging as Marker of Lipid Core in Middle Cerebral Artery Atherosclerosis

Wen-Jie Yang, PhD; Xiang-Yan Chen, PhD; Hai-Lu Zhao, PhD; Chun-Bo Niu, MD; Bing Zhang, MD, PhD; Yun Xu, MD, PhD; Ka-Sing Wong, MD; Ho-Keung Ng, MD

Background and Purpose—High signal on T1-weighted fat-suppressed images in middle cerebral artery plaques on ex vivo magnetic resonance imaging was verified to be intraplaque hemorrhage histologically. However, the underlying plaque component of low signal on T1-weighted fat-suppressed images (LST1) has never been explored. Based on our experience, we hypothesized that LST1 might indicate the presence of lipid core within intracranial plaques.

Methods—1.5 T magnetic resonance imaging was performed in the postmortem brains to scan the cross sections of bilateral middle cerebral arteries. Then middle cerebral artery specimens were removed for histology processing. LST1 presence was identified on magnetic resonance images, and lipid core areas were measured on the corresponding histology sections.

Results—Total 76 middle cerebral artery locations were included for analysis. LST1 showed a high specificity (96.9%; 95% confidence interval, 82.0%–99.8%) but a low sensitivity (38.6%; 95% confidence interval, 24.7%–54.5%) for detecting lipid core of all areas. However, the sensitivity increased markedly (81.2%; 95% confidence interval, 53.7%–95.0%) when only lipid cores of area ≥ 0.80 mm² were included. Mean lipid core area was 5× larger in those with presence of LST1 than in those without (1.63 ± 1.18 mm² versus 0.32 ± 0.31 mm²; $P=0.003$).

Conclusions—LST1 is a promising imaging biomarker of identifying intraplaque lipid core, which may be useful to distinguish intracranial atherosclerotic disease from other intracranial vasculopathies and to assess plaque vulnerability for risk stratification of patients with intracranial atherosclerotic disease. In vivo clinical studies are required to explore the correlation between LST1 and clinical outcomes of patients with intracranial atherosclerotic disease. (*Stroke*. 2016;47:2299-2304. DOI: 10.1161/STROKEAHA.116.013398.)

Key Words: atherosclerosis ■ lipid core ■ MCA ■ MRI ■ vessel wall imaging

Intracranial atherosclerotic disease (ICAD), especially in the middle cerebral artery (MCA), is an important cause of ischemic stroke in Asian, African-American, and Hispanic populations.¹ The severe atherosclerotic stenosis was demonstrated as an independent predictor for stroke recurrence in WASID trial (Warfarin Versus Aspirin for Symptomatic Intracranial Disease).² However, the independent role of percent stenosis in predicting subsequent stroke risk has been challenged in recent studies.³ Based on a series of autopsy of Chinese adults, we verified that both luminal stenosis caused by atherosclerotic plaque and percentage of lipid area, as well as the presence of intraplaque neovasculature, contribute to

the occurrence of ischemic stroke.⁴ Therefore, beyond the maximal luminal stenosis, the other features reflecting the characteristics of ICAD, such as plaque morphology and components, might be new promising markers in risk stratification of patients with ICAD.⁵

Accumulating evidence from clinical trials by using high-resolution magnetic resonance imaging (MRI) demonstrated that high signal on T1-weighted fat-suppressed images of MCA plaques is associated with ipsilateral stroke.⁶ High signal on T1-weighted fat-suppressed image within one MCA plaque in ex vivo MRI was verified to be intraplaque hemorrhage histologically.⁷ However, the clinical relevance of

Received March 8, 2016; final revision received June 8, 2016; accepted June 13, 2016.

From the Department of Medicine and Therapeutics (W.-J.Y., X.-Y.C., K.-S.W.) and Department of Anatomical and Cellular Pathology (H.-K.N.), Chinese University of Hong Kong, Shatin, Hong Kong SAR, China; Centre for Diabetic Systems Medicine, Guangxi Key Laboratory of Excellence, Guilin Medical University, Guilin, China (H.-L.Z.); Department of Pathology, China-Japan Union Hospital Affiliated to Jilin University, China (C.-B.N.); and Department of Radiology (B.Z.) and Department of Neurology (Y.X.), Affiliated Drum Tower Hospital of Nanjing University Medical School, China.

Guest Editor for this article was Tatjana Rundek, MD, PhD.

Presented in part at the International Stroke Conference, Los Angeles, CA, February 17–19, 2016.

Correspondence to Xiang-Yan Chen, PhD, Department of Medicine and Therapeutics, Chinese University of Hong Kong, Prince of Wales Hospital, Shatin, NT, Hong Kong, SAR, China. E-mail fionachen@cuhk.edu.hk

© 2016 The Authors. *Stroke* is published on behalf of the American Heart Association, Inc., by Wolters Kluwer. This is an open access article under the terms of the [Creative Commons Attribution Non-Commercial-NoDerivs](https://creativecommons.org/licenses/by-nc-nd/4.0/) License, which permits use, distribution, and reproduction in any medium, provided that the original work is properly cited, the use is noncommercial, and no modifications or adaptations are made.

Stroke is available at <http://stroke.ahajournals.org>

DOI: 10.1161/STROKEAHA.116.013398

low signal on T1-weighted fat-suppressed images (LST1) within intracranial vessel walls has never been reported till now. Based on our previous experience on ICAD,^{4,7-9} we hypothesized that LST1 should indicate the presence of lipid core within the plaques. With the similar design as reported recently,¹⁰ an ex vivo 1.5-T MRI-histology comparative study was performed to investigate the clinical implications of LST1 within intracranial atherosclerotic plaques.

Specimens and Methods

Specimens

Subjects for this study were drawn from the previous study comparing 1.5-T MRI with histology.^{8,10} The study was approved by the Clinical Research Ethics Committee of the Chinese University of Hong Kong. We consecutively recruited Chinese autopsy cases aged ≥ 45 years who died at the Prince of Wales Hospital, Hong Kong (a regional general hospital), during a period from December 2003 to June 2005. Postmortem MRI was performed to scan the cross-sections of bilateral MCAs. Among the cases with past history of stroke, uncommon causes of stroke, such as carotid dissection, hypercoagulable state, and vasculitis, were excluded. In addition, the cases with poor imaging quality or missing histology results were excluded.

The aim of this project was to identify whether the frequency of LST1 on MRI was consistent with a proportion of lipid core assessed on histology. Chi-square test of independence in 2-way contingency tables was used. Set w (effect size) = 0.4, power = 0.8, alpha = 0.05, df (degree of freedom) = $(2-1) \times (2-1) = 1$, then the sample size should be 50. In consideration of around 10% of lost cases because of poor quality of magnetic resonance (MR) images or sample damage during histology process according to our previous study, at least 55 patients would be needed.

The whole brain was obtained fresh and intact during the process of autopsies. The bilateral MCAs were washed with water to clear the possible blot inside. Then the whole brain was fresh-frozen at 4°C until imaged. The period between autopsy and imaging was <5 days.

MRI Protocol

The MRI examinations of the brains were performed by a 1.5-T scanner (Sonata, Siemens Medical Systems, Erlangen, Germany) with a standard 8-channel head coil. To keep the arteries uncollapsed, diluted barium solution was injected into the lumen to distend the artery. Then the brains were positioned in the scanner to resemble a supine head first position in routine clinical scanning. The orientation of the MCA was localized by the T2 sequence of the whole brain. An experienced radiologist would then choose an imaging plane perpendicular to each MCA to obtain the cross-sectional image of bilateral M1 arteries. Fat-suppressed T1-weighted and T2-weighted sequence was performed. Fat suppression technique was used to reduce fat signal. The parameters are as follows: repetition time (TR) 3000 ms; echo time (TE), 19 ms and 130 ms; excitation, 2; matrix, 179×256; field of view, 170 mm; slice thickness, 3 mm with no gap; and time of acquisition, 3 minutes 41 seconds. The resultant in-plane resolution was, therefore, 0.66×0.95 mm.

Image Review

Before review, an image quality rating for each contrast weighting was assigned to all MR images based on the overall signal-to-noise ratio and the clarity of vessel wall boundaries (4-point scale: 1=poor, 4=excellent). Images with an image quality ≤ 2 were excluded from the study.

Two investigators (Drs Zhang and Yang) who were blinded to the histology findings independently reviewed the images. With the gray matter adjacent to the plaque as the reference tissue, the signal intensity of the plaque was classified as iso-intensity and heterogeneous signal intensity, such as hyper-iso, iso-hypo, and hyper-hypo intensity. The LST1 was recorded as positive or negative. All the qualitative assessment data from both reviewers (Drs Zhang and Yang) were used to calculate the inter-rater reliability. To assess intrarater reliability, all images which were presented in a different order were re-evaluated 4 months after the initial review by 1 reviewer (Dr Yang).

The maximum and minimum wall thicknesses were then measured using Image-Pro Plus software (Media Cybernetics, Silver Spring). The eccentricity index was defined as (maximum wall thickness–minimum wall thickness)/maximum wall thickness. A lesion was defined as eccentric if the index was ≥ 0.5 and as concentric if < 0.5 , according to our previous study.¹⁰

Histological Processing and Analysis

Bilateral MCAs were removed after MRI scanning for histopathologic processing. The main trunks of bilateral MCAs (ie, M1) were removed intact from the brain and sectioned into blocks. The specimen was cut into 2-cm blocks, starting from the proximal and progressing distally toward the bifurcation, until the whole length of the specimen had been cut. Serial sections of MCAs were cut at 4-mm intervals. The specimens were processed and embedded in paraffin, and thereafter, 5- μ m-thick sections were cut and stained with hematoxylin-eosin.

Two pathologists (Drs Zhao and Niu) who were blinded to clinical data observed the histological sections from all segments. According to the revised American Heart Association criteria by Virmani et al,¹¹ plaques were assigned the following categories: early atherosclerotic lesions like intimal xanthoma and adaptive intima thickening, as well as advanced atherosclerotic lesions, such as pathological intima thickening, fibrous cap atheroma, thin fibrous cap atheroma, and fibrocalcific plaque. Because the size of MCA is incomparable to that of coronaries, the definition of thin fibrous cap atheroma derived from Virmani et al (fibrous cap < 65 μ m thick) could not be directly applied to our cases. Instead, we used the median thickness from the luminal border of the lipid core to the lumen as a reference according to a previous study; plaques with fibrous cap thickness below the median were defined as thin fibrous cap atheroma.¹²

Finally, the histology sections were photographed with a Leica DC 200 digital microscope. The area of lipid core (mm²) and distance from the lipid core to the lumen (mm) were manually measured 3 times by using Image-Pro Plus software, and the values were averaged. To assess inter-rater reproducibility, histology sections of 10 randomly selected subjects were re-evaluated by another reviewer.

Correlation Between MRI and Histology

After both MR images and histological sections were reviewed and categorized, histological sections were matched to the MR images based on the relative distance from the bifurcation of internal cerebral artery and MCA. To account for fixation-related shrinkage, the gross morphological features (ie, lumen, wall size and shape, appearance, and location of large calcifications) of the vessel wall were used to assist in matching the sections with each MR image location.

In view of the low signal-to-noise ratio of 1.5-T MRI and the impact of mismatch between MRI and histology, we used the artery as the unit of observation by choosing only one MCA location that was involved in atherosclerotic plaque and had good MR image quality per artery. In total, 76 MR image locations (1 location per artery; 1–2 MCAs per subject) were matched and compared with the corresponding histological sections.

Statistical Analysis

All data analyses were conducted using the SPSS 20.0 software package (SPSS, Inc). To compare the clinical characteristics between patients included in and excluded from the present study, the independent-samples *t* test and Fisher exact test were used for continuous and categorical data, respectively. Chi-square test was used to determine the association of the pattern of intima thickening (concentric versus eccentric) and detection of necrotic core. Independent-samples *t* test was used to compare the area of lipid core and distance from lipid core to lumen between the 2 groups. Using the histology results as the gold standard, sensitivity, specificity, positive and negative predictive value, Cohen’s κ , and Chi-square were calculated to evaluate the ex vivo accuracy of the MRI for detecting intraplaque lipid core. Receiver-operating curve analysis was performed to determine the lipid core size being predictive of correctly identifying the presence or absence of lipid core on MR images. To determine the inter- and intraobserver agreements, Cohen’s κ with 95% confidence intervals (CIs) was calculated for dichotomous data, and intraclass correlation coefficients (ICC) with a 1-way random effect and a 2-way random effect were calculated for intra- and interobserver continuous variables, respectively. A value of *P* <0.05 was considered to be statistically significant.

Results

Among the 61 original patients scanned, 14 were excluded from the study during image review as a result of overall poor image quality secondary to too much air in the arterial lumen, resulting in image artifacts (7 patients); inaccurate orientation of MRI scanning (3 patients); improper location of brain within the head coil (2 patients); and lack of corresponding histology sections (2 patients). Among the remaining 47 patients available for analysis, 26 (55.3%) were men with a mean age of 76 years. Eighteen (38.3%) patients had ischemic stroke and 13 (27.7%) showed brain infarct on MR images. The mean characteristics of the 47 patients are described in Table 1. The demographic and clinical characteristics were similar between the included and excluded patients (Table 1).

Among 94 arteries in 47 patients, 18 arteries were excluded because of image artifact (14 arteries) and lack of corresponding histology sections (4 arteries), leaving 76 locations (1 location per artery; 1–2 MCAs per subject) for further detailed analysis. Iso-intensity was detected on 22 vessels (28.9%) and heterogeneous signal intensity on the remaining 54 vessels, including hyper-iso intensity on 36 MCAs (47.4%), iso-hypo intensity on 4 vessels (5.3%), and hyper-hypo intensity on 14 MCAs (18.4%). Intraobserver agreement was almost perfect ($\kappa=0.88$ [0.78–0.96]), and interobserver agreement was substantial ($\kappa=0.80$ [0.67–0.92]) for the identification of T1 intensity.

Table 2 showed the changes of signal intensity on fat-suppressed T1-weighted MRI of intracranial atherosclerotic plaques classified as different phenotypes. Of 22 atherosclerotic lesions presenting with iso-intensity, 15 (68.2%) exhibited to be normal or early atherosclerotic lesions; the other 7 (31.8%) lesions showed advanced lesions. Heterogeneous signal intensity was found in 3 (5.6%) samples exhibiting early lesions and 51 (94.4%) showing advanced lesions. Figure 1 showed the representative MR images and corresponding histology.

Of the 76 MCA locations, 44 (57.9%) were found to have an underlying lipid core on histology, comprising 22 fibrous cap atheroma, 17 thin fibrous cap atheroma, and 5 fibrocalcific plaque. LST1 was identified on 18 (23.7%) MCA locations, 17 of which were confirmed to be intraplaque lipid core histologically (*P*<0.001). The sensitivity and specificity of LST1 for diagnosing lipid core of all areas were 38.6% (95% CI, 24.7%–54.5%) and 96.9% (95% CI, 82.0%–99.8%), respectively (Table 3). Revealed by receiver-operating curve analysis, the sensitivity and specificity were 81.2% (95% CI, 53.7%–95.0%) and 91.7% (95% CI, 80.9%–96.9%), respectively, when the cutoff of lipid core area for identifying the presence or absence of LST1 was set at 0.8 mm², resulting in a Cohen’s κ value of 0.70 (95% CI, 0.47–0.87; Table 3).

As shown in Figure 2, the mean area of lipid core assessed by histology was ≈5 times larger in the LST1 group than in

Table 1. Demographic and Clinical Data for Included and Excluded Patients

	Included (n=47)*	Excluded (n=14)*	PValue
Age, y	76±13	71±14	0.297
Males	26 (55.3%)	6 (42.9%)	0.545
Smoker	18 (38.2%)	3 (21.4%)	0.607
Hypertension	20 (42.6%)	5 (35.7%)	0.762
Diabetes mellitus	13 (27.7%)	4 (28.6%)	1.000
Atrial fibrillation	7 (14.9%)	3 (21.4%)	0.683
Hyperlipidemia	1 (2.1%)	1 (7.1%)	0.409
Ischemic heart disease	16 (34.0%)	5 (35.7%)	1.000
Hemorrhagic stroke	7 (14.9%)	2 (14.3%)	1.000
Ischemic stroke	18 (38.3%)	3 (21.4%)	0.342
Brain infarct	13 (27.7%)	4 (28.6%)	1.000

*Mean±SD or number (%).

Table 2. Signal Intensity on Fat-Suppressed T1-Weighted MRI of Intracranial Atherosclerotic Plaques Classified as Different Atherosclerotic Phenotypes

Atherosclerotic Phenotype	Isointensity	Heterogeneous Signal Intensity			Total
		Hyper-Iso	Iso-Hypo	Hyper-Hypo	
Normal or early lesions	15 (68.2%)	3 (5.6%)			
Normal	1 (4.5%)	0 (0.0%)	0 (0.0%)	0 (0.0%)	1
Intimal xanthoma	8 (36.4%)	1 (2.8%)	0 (0.0%)	0 (0.0%)	9
Adaptive intimal thickening	6 (27.3%)	2 (5.6%)	0 (0.0%)	0 (0.0%)	8
Advanced lesions	7 (31.8%)	51 (94.4%)			
Pathological intimal thickening	3 (13.6%)	10 (27.8%)	1 (25.0%)	0 (0.0%)	14
Fibrous cap atheroma	2 (9.1%)	13 (36.1%)	2 (50.0%)	5 (35.7%)	22
Thin fibrous cap atheroma	2 (9.1%)	8 (22.2%)	1 (25.0%)	6 (42.9%)	17
Fibrocalcific plaque	0 (0.0%)	2 (5.6%)	0 (0.0%)	3 (21.4%)	5
Total	22	36	4	14	76

MRI indicates magnetic resonance imaging.

the without LST1 group among the 44 patients with lipid core present ($1.63 \pm 1.18 \text{ mm}^2$ versus $0.32 \pm 0.31 \text{ mm}^2$; $P=0.003$). But the mean distance from the lipid core to the lumen showed no significant difference between the 2 groups ($0.26 \pm 0.10 \text{ mm}$ versus $0.25 \pm 0.11 \text{ mm}$; $P=0.788$). The intrarater reproducibility was excellent for the quantitative area measurements (ICC=0.98 [0.96–0.99]) and distance measurements (ICC=0.88 [0.80–0.93]); inter-rater reproducibility was substantial for the area (ICC=0.79 [0.46–0.93]) and distance measurements (ICC=0.74 [0.37–0.91]).

According to the eccentricity index, 45 (59.2%) lesions were identified as concentric and 31 (40.8%) plaques as eccentric while on MR images. The prevalence of lipid core

in eccentric and concentric lesions was 74.2% (23/31) and 46.7% (21/45), respectively ($P=0.017$). Considering only locations with lipid core, eccentric lesions had larger area of lipid core compared with concentric lesions ($1.20 \pm 1.20 \text{ mm}^2$ versus $0.42 \pm 0.45 \text{ mm}^2$; $P=0.007$).

Discussion

To our knowledge, this is the first study demonstrating the capability of ex vivo MR vessel wall imaging to identify intraplaque lipid within intracranial atherosclerosis. After comparison with histology findings, LST1 is verified to be lipid core within advanced atherosclerotic lesions, which may be used to differentiate ICAD from other etiologies causing intracranial arterial stenosis, such as Moyamoya disease or vasculitis.

Current imaging modalities, such as transcranial Doppler, magnetic resonance angiography, and digital subtraction angiography, which are capable of evaluating the arterial lumen status of intracranial vessels, cannot delineate the etiologies causing similar arterial occlusive disease.³ Detailed visualization of vessel wall changes may help to identify ICAD from other intracranial vasculopathies causing arterial stenosis, which may optimize personalized therapy in individual patients.¹³ Assuming that intracranial atherosclerosis pathophysiology parallels that in the carotid artery, plaque eccentricity is used as a criterion to differentiate between ICAD and other vasculopathies within brain vasculature in high-resolution MRI-related studies.¹⁴ In this study, however, more than half of the intracranial atherosclerotic lesions presented as concentric rather than eccentric intima thickening, which was consistent with our recent report on the same series of autopsy cases.¹⁰ Therefore, other imaging biomarkers rather than pattern of intima thickening should be developed to distinguish ICAD from other intracranial arterial disease.

Atherosclerosis is a progressive inflammatory disease¹⁵ initiated by endothelial injury and followed by cholesterol accumulation in the endothelial cells of the arterial wall.¹⁶ The formation of lipid core is a landmark of atherosclerosis maturation, and the extent may affect plaque stability and subsequent plaque rupture.¹⁷ Our previous postmortem study

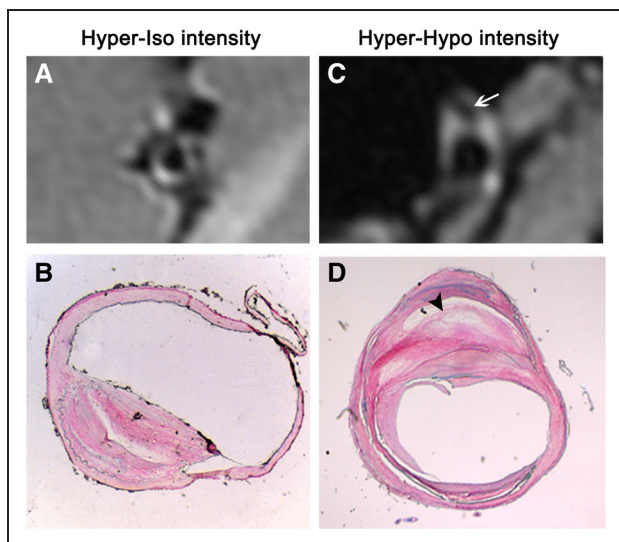


Figure 1. Representative magnetic resonance (MR) images of atherosclerotic plaque and their corresponding histopathologic sections. Fat-suppressed T1-weighted image (A) reveals a hyper-iso intensity plaque, which is suggestive as a fibrous cap atheroma (B). Fat-suppressed T1-weighted image (C) indicates a hyper-hypo intensity plaque, which is classified into thin fibrous atheroma on matched histological image (D). Area with low signal on MR image (arrow in C) is verified to be lipid core on corresponding histopathologic section (arrowhead in D).

Table 3. Sensitivity, Specificity, Positive, and Negative Predictive Value and Cohen's κ of the Low Signal on T1-Weighted Fat-Suppressed Images (LST1) to Detect Lipid Core, Grouped by Underlying Lipid Core Area Assessed by Histology

	Lipid Core	
	All Areas (n=44)	Areas ≥ 0.8 mm ² (n=16)
Sensitivity (95% CI)	38.6 (24.7–54.5)	81.2 (53.7–95.0)
Specificity (95% CI)	96.9 (82.0–99.8)	91.7 (80.9–96.9)
Positive predictive value (95% CI)	23.7 (15.0–35.1)	23.7 (15.0–35.0)
Negative predictive value (95% CI)	76.3 (64.9–85.0)	76.3 (64.9–85.0)
Cohen's κ (95% CI)	0.32 (0.16–0.49)	0.70 (0.47–0.87)

CI indicates confidence interval.

showed that the percentage of lipid area within MCA vessel walls, in addition to luminal stenosis and intraplaque neovasculature, plays a key role in leading to brain infarctions in the corresponding territory.⁴ Accordingly, the identification of lipid components within intracranial vessel wall lesions may help to distinguish ICAD from other arterial diseases.

Based on this 1.5-T MRI-histology comparative study, LST1 showed high sensitivity (81.2%) and high specificity (91.7%) in identifying lipid cores of area ≥ 0.80 mm² within MCA atherosclerotic plaques, indicating that LST1 is a promising imaging biomarker for identifying intraplaque lipid core. The sensitivity decreased markedly if area < 0.80 mm² were included (36.8%), which is most likely attributable to the inferior spatial resolution of 1.5 T MRI. Accordingly, the mean area of lipid core assessed by histology was ≈ 5 times larger in the LST1 group than in the without LST1 group, suggesting that LST1 was more reliable in detecting lipid core of larger area.

Although the capability of high-resolution MRI in identifying plaque components has been validated by using carotid artery specimens from carotid endarterectomy, the application

of high-resolution MRI in assessing intracranial arterial disease requires to be validated by histological evidences. Our present ex vivo study provides limited but valuable histology evidence in assisting signal interpretations of MRI vessel wall imaging.¹⁸ Similar to our study, the capability of 7.0-T MRI identifying plaque components occurring within intracranial large arteries was reported in identifying fibrotic components (hyperintense signal), calcium deposition (hypointense signal), and areas of foamy macrophages (hypointense areas).^{19,20} Comparably, the strength of our present study lies in increased sample size to verify the sensitivity and specificity of low signal in identifying intracranial lipid core. LST1 within intracranial vascular lesions may serve as a new imaging biomarker to distinguish ICAD from other intracranial arterial disease. The relationship between pattern of intima thickening and detection of lipid core indicates that the eccentric lesions tend to contain greater prevalence and larger area of lipid core compared with concentric lesions, implying that the vessel wall MRI may perform better on eccentric plaques within brain vasculature. In vivo clinical studies are required to explore the correlation between LST1 and clinical outcomes of stroke patients with ICAD.

This study has some limitations. First, like the other ex-vivo imaging studies, the signal characteristics on ex-vivo MRI imaging could not totally reflect the intracranial vessel wall changes in living patients because of a potential change in tissue contrast resulting from tissue degradation and dehydration.²¹ However, our findings from this ex-vivo MRI-histology comparative study may deepen our understanding about the pathology of ICAD and partly fill in the gaps between histology and imaging features because of lack of cerebral artery specimens. Second, pathological examination of the matched MCA specimens was used as the gold standard for evaluating the plaque components on MR images. However, the areas of lipid core could be underestimated because of specimen shrinkage during the fixation and subsequent dehydration and embedding procedure. Shrinkage of arterial rings specimens were reported to be on average 19% to 25% in area,²² 15% in width, and

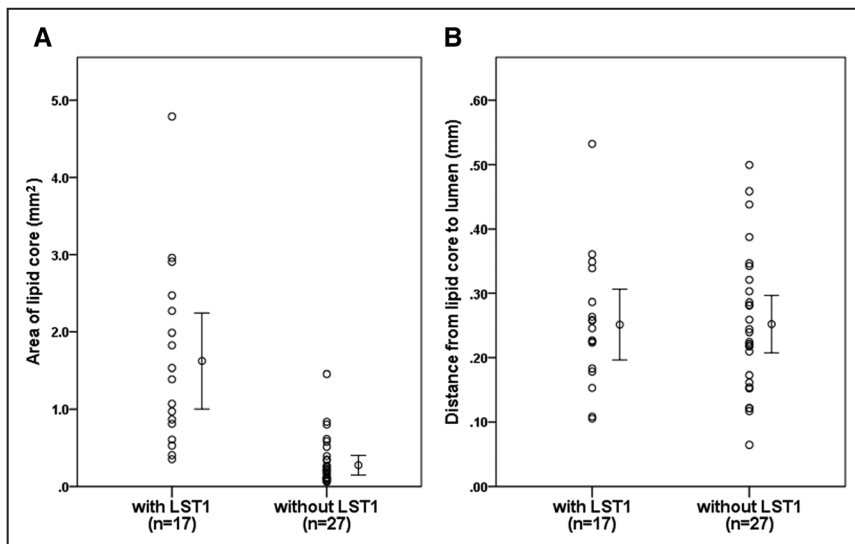


Figure 2. A, Area of lipid core assessed by histological slides comparing low signal on T1-weighted fat-suppressed images (LST1) and without LST1 in the locations with lipid core. Lipid core area is significantly larger in the plaque with LST1 group than without LST1 group. **B,** Distance from lipid core to the lumen assessed by histological slides comparing LST1 and without LST1 in the locations with lipid core. Distance from lipid core to the lumen shows no difference in the plaque with LST1 group and without LST1 group.

30% in length²³ compared with ex vivo MRI, making the comparison of absolute values difficult. In further studies, the shrinkage distortions should be corrected by defining relative to total plaque area or by strain-based 3D reconstructions.²⁴ Finally, cautions should be taken when interpreting the signal density based on single fat-suppressed T1-weighted MRI sequence. Multiple MRI sequences, especially contrast-enhanced MRI, may help to improve the accuracy and reproducibility of tissue quantification. Additional studies are needed to validate the clinical significance of low signal on MR vessel wall imaging in live patients by modified scanning techniques.^{5,25,26}

To our knowledge, this is the first ex vivo MRI study to validate the signal characteristics caused by lipid core within intracranial atherosclerotic lesions by referring to histology. LST1 is a promising imaging biomarker of identifying intraplaque lipid core, which may be useful to distinguish ICAD from other intracranial vasculopathies and to assess plaque vulnerability for risk stratification of patients with ICAD.

Acknowledgments

We thank our research assistant Mr Leung Kam Tat for his assistance in statistical analysis.

Sources of Funding

This work was supported by the funding from the Chinese University of Hong Kong (Focused Investment Scheme B) and Lui Che Woo Institute of Innovative Medicine (LCW IIM), the Chinese University of Hong Kong.

Disclosures

None.

References

- Gorelick PB, Wong KS, Bae HJ, Pandey DK. Large artery intracranial occlusive disease: a large worldwide burden but a relatively neglected frontier. *Stroke*. 2008;39:2396–2399. doi: 10.1161/STROKEAHA.107.505776.
- Kasner SE, Chimowitz MI, Lynn MJ, Howlett-Smith H, Stern BJ, Hertzberg VS, et al; Warfarin Aspirin Symptomatic Intracranial Disease Trial Investigators. Predictors of ischemic stroke in the territory of a symptomatic intracranial arterial stenosis. *Circulation*. 2006;113:555–563. doi: 10.1161/CIRCULATIONAHA.105.578229.
- Leng X, Wong KS, Liebeskind DS. Evaluating intracranial atherosclerosis rather than intracranial stenosis. *Stroke*. 2014;45:645–651. doi: 10.1161/STROKEAHA.113.002491.
- Chen XY, Wong KS, Lam WW, Zhao HL, Ng HK. Middle cerebral artery atherosclerosis: histological comparison between plaques associated with and not associated with infarct in a postmortem study. *Cerebrovasc Dis*. 2008;25:74–80. doi: 10.1159/000111525.
- Bodley JD, Feldmann E, Swartz RH, Rumboldt Z, Brown T, Turan TN. High-resolution magnetic resonance imaging: an emerging tool for evaluating intracranial arterial disease. *Stroke*. 2013;44:287–292. doi: 10.1161/STROKEAHA.112.664680.
- Xu WH, Li ML, Gao S, Ni J, Yao M, Zhou LX, et al. Middle cerebral artery intraplaque hemorrhage: prevalence and clinical relevance. *Ann Neurol*. 2012;71:195–198. doi: 10.1002/ana.22626.
- Chen XY, Wong KS, Lam WW, Ng HK. High signal on T1 sequence of magnetic resonance imaging confirmed to be intraplaque haemorrhage by histology in middle cerebral artery. *Int J Stroke*. 2014;9:E19. doi: 10.1111/ijvs.12277.
- Chen XY, Lam WW, Ng HK, Zhao HL, Wong KS. Diagnostic accuracy of MRI for middle cerebral artery stenosis: a post-mortem study. *J Neuroimaging*. 2006;16:318–322. doi: 10.1111/j.1552-6569.2006.00048.x.
- Chen XY, Lam WW, Ng HK, Fan YH, Wong KS. The frequency and determinants of calcification in intracranial arteries in Chinese patients who underwent computed tomography examinations. *Cerebrovasc Dis*. 2006;21:91–97. doi: 10.1159/000090206.
- Yang WJ, Chen XY, Zhao HL, Niu CB, Xu Y, Wong KS, et al. In vitro assessment of histology verified intracranial atherosclerotic disease by 1.5T magnetic resonance imaging: concentric or eccentric? *Stroke*. 2016;47:527–530. doi: 10.1161/STROKEAHA.115.011086.
- Virmani R, Kolodgie FD, Burke AP, Farb A, Schwartz SM. Lessons from sudden coronary death: a comprehensive morphological classification scheme for atherosclerotic lesions. *Arterioscler Thromb Vasc Biol*. 2000;20:1262–1275.
- Gutierrez J, Elkind MS, Virmani R, Goldman J, Honig L, Morgello S, et al. A pathological perspective on the natural history of cerebral atherosclerosis. *Int J Stroke*. 2015;10:1074–1080. doi: 10.1111/ijvs.12496.
- Holmstedt CA, Turan TN, Chimowitz MI. Atherosclerotic intracranial arterial stenosis: risk factors, diagnosis, and treatment. *Lancet Neurol*. 2013;12:1106–1114. doi: 10.1016/S1474-4422(13)70195-9.
- Ryoo S, Lee MJ, Cha J, Jeon P, Bang OY. Differential vascular pathophysiology types of intracranial atherosclerotic stroke: a high-resolution wall magnetic resonance imaging study. *Stroke*. 2015;46:2815–2821. doi: 10.1161/STROKEAHA.115.010894.
- Fuster V, Badimon JJ, Chesebro JH. Atherothrombosis: mechanisms and clinical therapeutic approaches. *Vasc Med*. 1998;3:231–239.
- Yatsu FM, Fisher M. Atherosclerosis: current concepts on pathogenesis and interventional therapies. *Ann Neurol*. 1989;26:3–12. doi: 10.1002/ana.410260102.
- Finn AV, Nakano M, Narula J, Kolodgie FD, Virmani R. Concept of vulnerable/unstable plaque. *Arterioscler Thromb Vasc Biol*. 2010;30:1282–1292. doi: 10.1161/ATVBAHA.108.179739.
- Turan TN, Rumboldt Z, Granholm AC, Columbo L, Welsh CT, Lopes-Virella MF, et al. Intracranial atherosclerosis: correlation between in-vivo 3T high resolution MRI and pathology. *Atherosclerosis*. 2014;237:460–463. doi: 10.1016/j.atherosclerosis.2014.10.007.
- Majidi S, Sein J, Watanabe M, Hassan AE, Van de Moortele PF, Suri MF, et al. Intracranial-derived atherosclerosis assessment: an in vitro comparison between virtual histology by intravascular ultrasonography, 7T MRI, and histopathological findings. *AJNR Am J Neuroradiol*. 2013;34:2259–2264. doi: 10.3174/ajnr.A3631.
- van der Kolk AG, Zwanenburg JJ, Denswil NP, Vink A, Spliet WG, Daemen MJ, et al. Imaging the intracranial atherosclerotic vessel wall using 7T MRI: initial comparison with histopathology. *AJNR Am J Neuroradiol*. 2015;36:694–701. doi: 10.3174/ajnr.A4178.
- Cai J, Hatsukami TS, Ferguson MS, Kerwin WS, Saam T, Chu B, et al. In vivo quantitative measurement of intact fibrous cap and lipid-rich necrotic core size in atherosclerotic carotid plaque: comparison of high-resolution, contrast-enhanced magnetic resonance imaging and histology. *Circulation*. 2005;112:3437–3444. doi: 10.1161/CIRCULATIONAHA.104.528174.
- Dobrin PB. Effect of histologic preparation on the cross-sectional area of arterial rings. *J Surg Res*. 1996;61:413–415. doi: 10.1006/jsre.1996.0138.
- Eubank W, Yuan C, Fisher E, Luna J, Reichenbach D, Schmiedl U, et al. Endarterectomy plaque shrinkage: comparison of t2-weighted mr imaging of ex vivo specimens to histologically processed specimens. *J Vasc Invest*. 1998;4:161–170.
- Lorraine Lowder M, Li S, Carnell PH, Vito RP. Correction of distortion of histologic sections of arteries. *J Biomech*. 2007;40:445–450. doi: 10.1016/j.jbiomech.2005.12.019.
- Mossa-Basha M, Hwang WD, De Havenon A, Hippe D, Balu N, Becker KJ, et al. Multicontrast high-resolution vessel wall magnetic resonance imaging and its value in differentiating intracranial vasculopathic processes. *Stroke*. 2015;46:1567–1573. doi: 10.1161/STROKEAHA.115.009037.
- Dieleman N, van der Kolk AG, Zwanenburg JJ, Hartevelde AA, Biessels GJ, Luijten PR, et al. Imaging intracranial vessel wall pathology with magnetic resonance imaging: current prospects and future directions. *Circulation*. 2014;130:192–201. doi: 10.1161/CIRCULATIONAHA.113.006919.